A Magnetic Field Transducer Based on Closed-Loop Operation of Magnetic Sensors

Gabriele GRANDI and Marco LANDINI
Dept. of Electrical Engineering, University of Bologna, 40136 - Italy
gabriele.grandi@mail.ing.unibo.it, marco.landini@mail.ing.unibo.it

Abstract - **A high sensitivity magnetic transducer able to sense magnetic fields from DC up to tens kHz is discussed in this paper. The system is based on a nulling field coil fed by a current on the basis of the residual field, sensed by a magnetic sensor (Hall or magneto-resistive) placed in the coil center. In this way, the coil current proportionally represents the external field component along the coil axis, and it can be easily converted in a voltage signal by a series resistor. Then, a one-axis gauss meter can be readily obtained. The sensitivity and the bandwidth of the overall system are discussed by a transfer function analysis. A hardware prototype has been realized, and significant test results are shown by means of a reference magnetic field generation set-up. Useful guidelines for the overall system design are given in the paper.**

I. INTRODUCTION

Recently, additional research and public attention have been focused on possible health effects of low frequency magnetic fields, with reference to low-level long-period human exposures. Furthermore, the measurement of magnetic field has become an important concern in industry over the past several years. As a consequence, the scientific and technical attention has been lead towards the development of apparatus and protocol to accurately sense and measure magnetic fields [1]. The challenge is to realize magnetic transducers, or gauss meters, having at the same time high sensitivity, good accuracy and wide bandwidth, with the additional requirement to be economically feasible.

Conventional field measurement technologies [2], [3] mainly include integrating flux meters (based on Faraday's law), fluxgate magnetometers [4], and open-loop magnetic sensors [5]. The use of Hall effect sensors and magneto-resistive devices has been recently encouraged by the development of hardware and software compensation blocks to improve the system accuracy. In fact, these sensing elements are inherently non-linear [6] and they are affected by field strength and temperature. Then, a thermistor is required as additional component. Various compensation methods have been considered, such as mathematical models and polynomial approximations. More recently, E-EPROM data storage [7] and artificial neural network [8] have been proposed. In general, these methods exhibit good results but require instrumentation amplifiers, digital signal processors, and a laborious tuning or learning process.

In order to overcome these drawbacks, a closed-loop magnetic transducer based on nulling the field across the magnetic sensor is considered in this paper. The current flowing in the nulling coil is driven by the sensor signal. In this way, the sensor is kept inside the control loop and, if the loop gain is high enough, the coil current is proportional to the magnetic field, regardless to the sensor non-linearities and temperature drifts. The transducer circuit is described with additional details in Section II whereas the transducer behavior is characterized in Section III by a transfer function analysis. In Section IV is summarized a comparison with respect to other magnetic transducers. Some practical results are presented in Section V, on the basis of an experimental set-up including a transducer prototype and a magnetic field generation system.

II. CIRCUIT DESCRIPTION

A simplified circuit diagram of the closed-loop magnetic field transducer is represented in Fig. 1. The magnetic sensor (Hall or magneto-resistive) is placed in the coil center. It produces a voltage v_s proportional by the open circuit sensitivity parameter K_s to the residual flux density along the coil axes, $\Delta B = B_{ext} - B_c$

$$v_s = K_s \, \Delta B \, . \tag{1}$$

The sensor voltage is amplified by an op-amp and then fed to a push-pull amplifier. The push-pull amplifier drives the coil current i_c in order to cancel the magnetic field in the coil center. The resulting working point, near zero field, eliminates the dependence on the linearity of the magnetic sensor and also reduces the temperature drift, as shown in the next Section. The output current can be converted to a voltage, v_m, by placing the measurement resistor R_m from the coil to ground.

The nulling coil consists in an air-core winding having N_c turns, with a coil resistance R_c and a coil inductance L_c. The relationship between the coil current i_c and the magnetic flux density B_c at the coil center is given by the field coefficient K_B, defined as

$$K_B = \frac{B_c}{i_c} \cong 0.4\pi \, \frac{N_c}{D_c} \, . \tag{2}$$

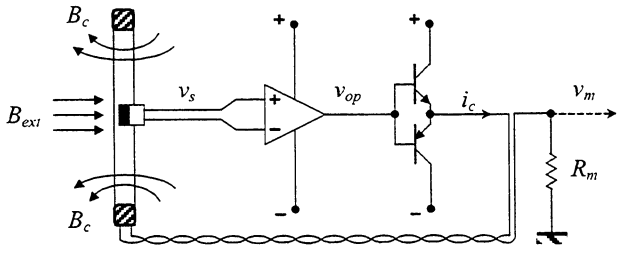

Fig. 1. Simplified circuit diagram of the system

0-7803-7369-3/02/$17.00 © 2002 IEEE

Eq. (2) is expressed in the case of a circular winding. If the coil diameter D_c is considered in mm, the field coefficient results in μT/mA.

III. Transfer Function Analysis

The block diagram of the overall system is represented in Fig. 2, assuming the nulling coil current i_c as the output and the external field B_{ext} as the input variable. The resulting closed-loop transfer function, representing a current sensitivity (mA/μT), can be expressed as

$$\frac{I_c(s)}{B_{ext}(s)} = S_I(s) = \frac{G(s)}{1+G(s)H(s)} = \frac{1}{H(s)+1/G(s)}, \quad (3)$$

where

$$G(s) = \frac{K_s\, G_{op}(s)}{R_m + R_c + s\,L_c} = \frac{K_s}{R_{tot}} \frac{G_{op}(s)}{(1+\tau_c\, s)}, \quad \tau_c = \frac{L_c}{R_{tot}} \quad (4)$$

$$H(s) = K_B. \quad (5)$$

It is assumed that the sensor bandwidth (that is usually the range of MHz) is much greater with respect to those of the other blocks. Then, the sensor dynamic is neglected and the corresponding sensor sensitivity K_s is treated as a real number. The op-amp can be considered as a first order system to represent its open-loop behavior

$$G_{op}(s) = \frac{K_{op}}{1+\tau_{op}\, s}, \quad (6)$$

where K_{op} is the static gain, and τ_{op} is the time constant (open-loop). Usually, τ_{op} is in the order of tens of ms, much greater than τ_c, that is in the order of tens of μs:

$$\tau_{op} >> \tau_c. \quad (7)$$

On the basis of (7) it can be assumed that the op-amp pole expressed in (6) dominates with respect to the coil pole in (4). Then, as a first order of approximation, the coil dynamic can be neglected, and (4) can be simplified as

$$G(s) \cong \frac{K_s K_{op}}{R_{tot}} \frac{1}{1+\tau_{op}\, s}. \quad (8)$$

Introducing (8) and (5) in (3), a simplified transfer function of the first order for the magnetic transducer is obtained

$$S_I(s) \cong \frac{1}{K_B + \frac{R_{tot}}{K_s K_{op}}(1+\tau_{op}\, s)}. \quad (9)$$

Eq. 9 can be rewritten in terms of static gain $S_I(0)$ and time constant τ of the overall system (closed-loop):

$$S_I(s) \cong \frac{S_I(0)}{1+\tau s}, \quad (10)$$

where

$$S_I(0) = \frac{1/K_B}{1+\frac{R_{tot}}{K_B K_s K_{op}}} \quad \text{and} \quad \tau = \frac{\tau_{op}}{1+\frac{K_B K_s K_{op}}{R_{tot}}}. \quad (11)$$

It will be show later that the loop static gain is

$$K_{tot} = G(0)H(0) = \frac{K_B K_s K_{op}}{R_{tot}} >> 1. \quad (12)$$

Then, (11) are further simplified as

$$S_I(0) \cong \frac{1}{K_B}, \quad \tau \cong \frac{\tau_{op}}{K_{tot}} \quad \text{or} \quad f_o \cong K_{tot} f_{op}. \quad (13)$$

The static and dynamic characteristics of the magnetic transducer are expressed by (10) and (13), and can be summarized in two main points:

- The static gain $S_I(0)$ represents the current sensitivity in terms of mA/μT. $S_I(0)$ is an inverse function of the field coefficient K_B, i.e., it depends on the geometrical characteristic of the nulling coil only.

As a consequence, $S_I(0)$ can be expressed by (2), regardless to non-linearity or thermal drift affecting the open circuit sensitivity coefficient K_s of the magnetic sensor.

- The cut-off frequency f_o, representing the bandwidth of the magnetic transducer, is K_{tot} times the open-loop one of the op-amp, f_{op}, as shown in (13).

In particular, (12) says that the lower is the total resistance R_{tot}, the higher is the bandwidth. On the other hand, the measuring resistance R_m should be high enough to have a good output voltage level.

The value of K_B should be chosen by a compromise also: it is advisable to be high enough to obtain a wide bandwidth, but it should be limited to have a good current sensitivity in terms of mA/μT.

The static gain can be represented in terms of output voltage sensitivity $S_V(0)$, expressed in mV/μT, as

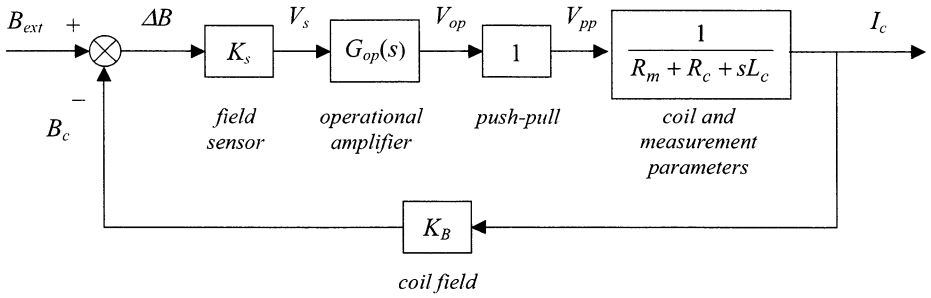

Fig. 2. Block diagram of the closed-loop magnetic transducer

$$S_V(0) = R_m S_I(0) \cong R_{tot} S_I(0) = \frac{R_{tot}}{K_B}. \quad (14)$$

Then, it is useful to introduce a "*gain-bandwidth product*" (GBP) for the transducer, as the product between the voltage sensitivity and the closed-loop cut-off frequency

$$GBP_V = S_V(0) \cdot f_o \cong \frac{R_{tot}}{K_B} \cdot K_{tot} f_{op} = K_s \cdot K_{op} f_{op}. \quad (15)$$

By introducing in (15) the GBP for the op-amp, yields

$$GBP_V \cong K_s \cdot GBP_{op}. \quad (16)$$

Eq. (16) states that the overall GBP_V of the closed-loop magnetic transducer is practically affected only by the open circuit sensitivity of the magnetic sensor, and the GPB of the op-amp. By changing all the other circuit parameters results in increase the sensitivity and corresponding decrease the bandwidth, or vice versa.

IV. Comparison with Respect to Other Magnetic Field Transducers

As known, the operating principle of integrating flux meters is based on the Faraday's law of induction. As a consequence, flux meters require a very stable integrator to obtain the magnetic field with a good accuracy, starting from the voltage induced on a coil probe. The main advantage of magnetic field transducers based on Hall-effect or magneto-resistive sensors with respect to integrating flux meters is the possibility to accurately sense extremely low frequency, including DC fields. In addition, magnetic sensor can be moved during the measurements, whereas the coil probe of the flux meters must stand still, to avoid induced voltage perturbations.

The main advantage of the proposed closed-loop transducer with respect to the open-loop ones is to overcome the problems related to the compensation of non-linear behavior and thermal drift of the magnetic sensor element. Then, the closed-loop system leads to higher stability, better accuracy and reduced costs.

On the other hand, the proposed system introduces a field perturbation in the region around the transducer, due to the compensating current through the nulling coil. In the case of circular coils shaped as a ring, it is possible to evaluate the disturbance filed B_d by considering the expression of the magnetic at the distance d far from a circular current loop

$$B_d \cong 0.05\pi D_c^2 \frac{N_c i_c}{d^3}, \quad (\mu T) \quad \text{with } d >> D_c. \quad (17)$$

Introducing (2) in (17), the ratio between the disturbance field B_d and the field B_o in the coil center, i.e., the measured one, can be determined

$$\frac{B_d}{B_o} \cong \frac{1}{8}\left(\frac{D_c}{d}\right)^3. \quad (18)$$

Eq. (18) shows that the relative field disturbance is about 0.1% at a distance d only five times greater than the coil diameter D_c.

An additional drawback of the closed-loop transducer is the alteration of the transducer sensitivity in presence of ferromagnetic objects in the close proximity of the nulling coil, owing to the variation of field coefficient K_B, as expressed by (2). Anyway, these perturbations are negligible if the distance of the ferromagnetic objects from the nulling coil is smaller with respect to their geometric dimensions.

V. Experimental Set-Up and Results

Significant experimental tests carried out on a prototype of the measuring system are presented in this Section. A practical realization of the closed-loop magnetic transducer is described in Subsection *A*, together with some practical considerations. A reference magnetic field generation system able to generate the testing field is described in Subsection *B*. The experimental results are presented in Subsection *C*, emphasizing the static and the dynamic characteristic of the magnetic transducer prototype.

A. Magnetic transducer prototype description

A magnetic transducer prototype has been realized on the basis of the specific guidelines given in Section III. Two windings with different turns number have been wound: the coil #1 has $N_c = 10$, the coil #2 has $N_c = 50$. The main geometric and electric parameters are given in Table I.

In order to emphasize the prototype behavior in its whole frequency range, it has been chosen to limit the bandwidth to few kHz, since the magnetic field generation system cover a frequency range up to 5 kHz (see the next Subsection *B*).

TABLE I
ELECTRIC AND GEOMETRIC PROTOTYPE PARAMETERS

Parameters	*Symbols*	*Values*	*Units*
Coils		#1 / #2	
Diameter	D_c	53 / 50.5	mm
Turns number	N_c	10 / 50	
Resistance	R_c	1.2 / 5.7	Ω
Inductance	L_c	12 / 280	μH
Op-amp characteristics (*rated, open-loop*)			
Cut-off frequency	f_{op}	25	Hz
Static gain	K_{op}	106	dB
Gain BW Product	GBP_{op}	5000	kHz
Circuit and sensor parameters (*rated*)			
Measuring resistance	R_m	100	Ω
Power supply	E_{dc}	± 12	V
Sensor type		magneto-resistive	
Open circuit sensitivity	K_s	0.045÷0.106	mV/μT
Frequency range	f_s	0 to 1M	Hz

TABLE II
STATIC AND DYNAMIC PROTOTYPE PARAMETERS

Parameters	*Symbols*	*Coil #1*	*Coil #2*	*Units*
Field coeff.	K_B	0.238	1.247	μT/mA
Loop gain	K_{tot}	21÷50	106÷250	
Cut-off freq.	f_o	0.5÷1.2	2.6÷6.2	kHz
Current sens.	$S_I(0)$	4.2	0.80	mA/μT
Voltage sens.	$S_V(0)$	420	80	mV/μT
GBP (voltage)	GBP_V	210÷500	210÷500	kHz mV/μT

In Table II are reported the main static and dynamic parameters of the magnetic transducer, calculated by the expression given in Section III.

Being the static gain of the op-amp high enough, it is verified that the loop static gain is $K_{tot} >> 1$, as previously stated in Section III. Then, the current sensitivity S_I (0) of the closed-loop magnetic transducer is only a function of the field coefficient K_B of the nulling coil.

B. Reference field generation system

A reference magnetic filed generation system has been realized in order to verify static and dynamic performance of the transducer prototype. The generation system consists in a single square loop wire having the side a of about 1m [9]. The wire is sustained by a solid wood structure, assembled with brass screws. The relationship between supply current i_s and flux density B_{ext} at the square center is

$$\frac{B_{ext}}{i_s} = \frac{0.8\sqrt{2}}{a} \cong 1.14\ \mu\text{T/A}. \tag{19}$$

The working zone is limited to the volume close to the square loop center, due to the non-uniform filed distribution. In particular, inside a 10 cm cube placed in the square loop center, the field deviation is lower than 1%. It has been analytically verified that the errors in the geometric dimensions affect the field accuracy less than 1%. Then, measuring the instantaneous value of the supply current it is possible to calculate the corresponding flux density by (19), with a good approximation [10].

The power supply is from by a HP 6834B Power Source / Analyzer, able to generate voltage waveform up to 5 KHz. All the supply wirings are twisted, and the power set-up is kept far form the square loop to avoid magnetic field interferences with respect to the working zone.

C. Experimental tests

In order to obtain significant tests, the transducer prototype has been placed in the central working zone of the reference field generation system, with the sensor/coil axis aligned with the square loop axis. All the system has been horizontally oriented so that the earth's magnetic field, i.e., about 35 μT in the Lab, resulted perpendicular to this common axis, to avoid the corresponding DC field offset. A simple high-pass filter can be also employed to cut-off the DC field components in the case of accurate ac magnetic field measurements.

The first test consists in verifying the transducer linearity by applying a 50 Hz sinusoidal field waveform having amplitude ranging from fractions to tens of μT. The results are shown in Fig. 3 for both the coils #1 and #2. The measured data are shown by dots (black and white, respectively), whereas the dashed lines represent the corresponding linear fitting. The voltage sensitivities (mV/μT) resulting from Fig. 3 confirm the calculated ones shown in Table II.

In Fig. 4 the frequency response (p.u.) of the magnetic field transducer is shown with reference to both coils #1 and #2. Also in this case, the measured data are shown by dots (black and white), whereas the dashed lines represent a fitting on the basis of transfer functions of the first order. The resulting cut-off frequencies f_o, representing the transducer bandwidth related to the two different coils, are 700 Hz and 3.45 kHz, respectively, well inside the calculated ranges shown in Table II.

The prototype behavior considering different flux density waveforms is shown from Fig. 5 to Fig. 7. The left column (a) concerns the coil #1, whereas the right column (b) concerns the coil #2. The waveforms of the magnetic flux density are represented on the basis of the voltage drop across a 0.47 Ω resistor connected in series with the current supping the reference field generation system. On the basis of (19), the resulting scaling factor is: 1.14 (μT/A) / 0.47 (Ω) ≅ 2.43 (μT/V).

Fig. 5 shows the sinusoidal steady-state behavior at low frequency (50 Hz), with field amplitude of about 2 μT. Fig. 6 and 7 show the prototype behavior in response to trapezoidal and rectangular field waveforms, respectively (400 Hz, 1.5 μT peak). The different transient performances are emphasized with reference to the different dynamic characteristics related to coil #1 and coil #2.

In general, all the experimental results show satisfactory performance for the closed-loop transducer, in good agreement with the theoretical predictions.

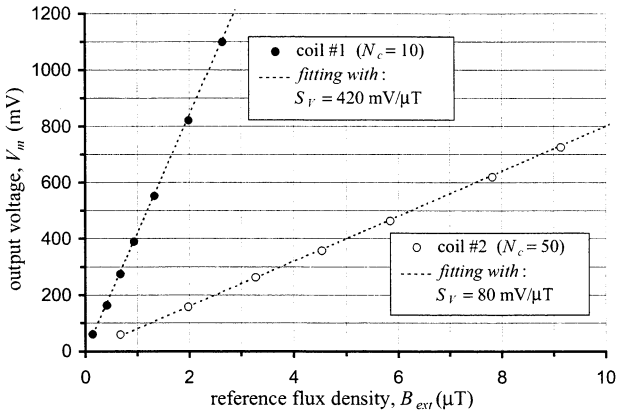

Fig. 3. Linearity test in sinusoidal steady-state (50 Hz): measured data (dots) and fitting (dashed lines)

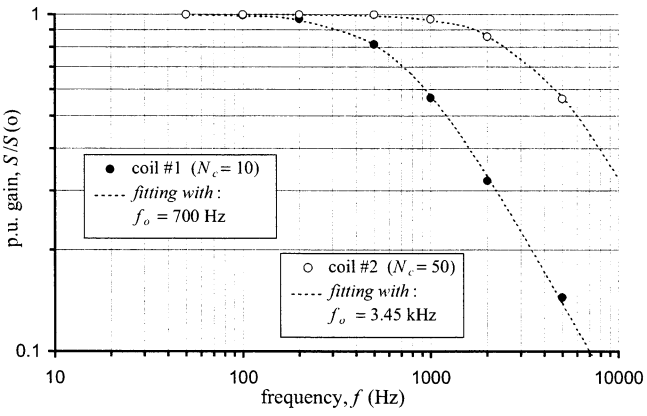

Fig. 4. Frequency response at B ≅ 2 μT (peak): measured data (dots) and fitting (dashed lines)

Behavior of the closed-loop magnetic transducer considering different flux density waveforms

(a) - Coil #1, N_c = 10 turns
upper traces: (1) reference field signal (2.43 μT/V)
lower traces: (2) output voltage, v_m (2.38 μT/V)

(b) - Coil #2, N_c = 50 turns
upper traces: (1) reference field signal (2.43 μT/V)
lower traces: (2) output voltage, v_m (12.5 μT/V)

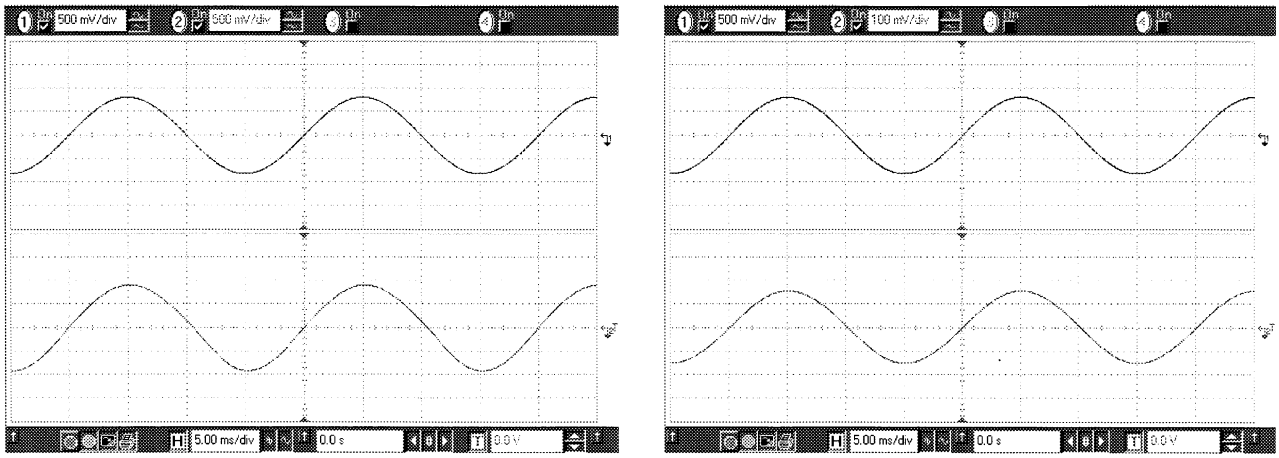

(a) Fig. 5. Sinusoidal steady-state (50 Hz) **(b)**

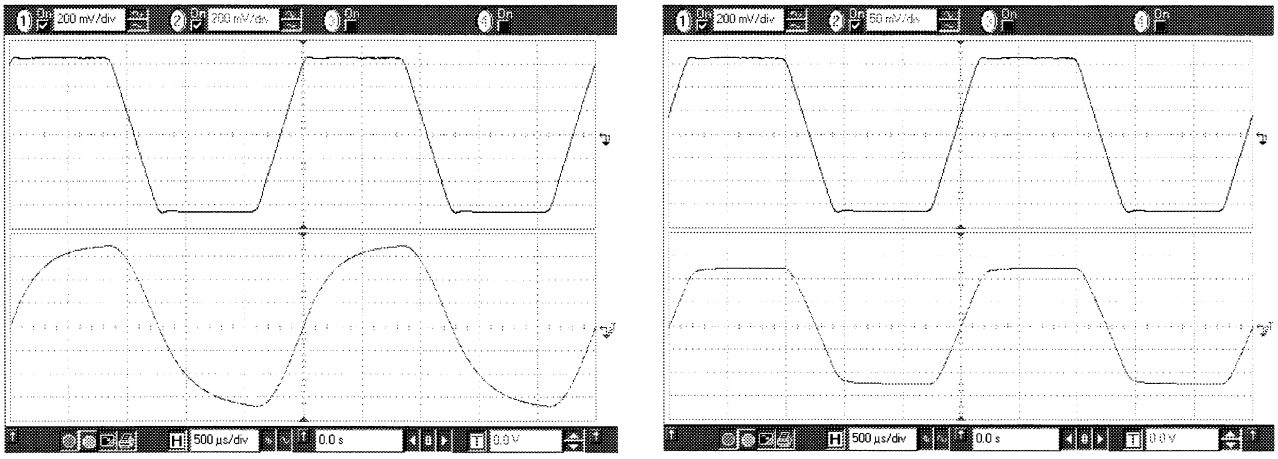

(a) Fig. 6. Trapezoidal field waveform (400 Hz) **(b)**

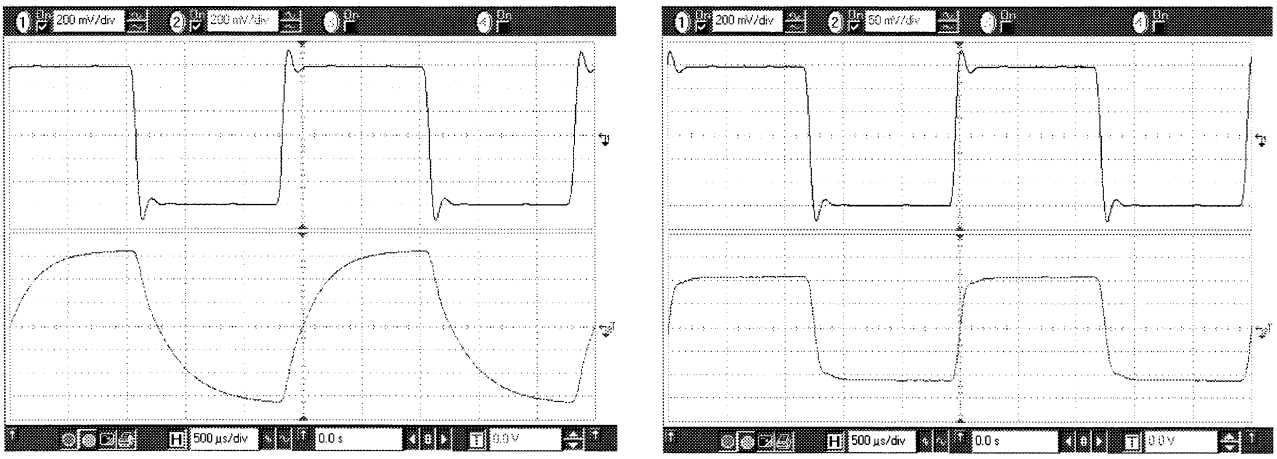

(a) Fig. 7. Rectangular field waveform (400 Hz) **(b)**

VI. Conclusion

A magnetic field transducer able to sense magnetic fields from DC up to tens kHz is discussed in this paper. The closed-loop operation allows to overcome the know problems of magnetic sensors in terms of non-linearity and thermal drift, avoiding additional hardware and software compensating blocks to be included in the measuring system.

The sensitivity and the bandwidth of the closed-loop transducer have been discussed by transfer function analysis, and a *gain-bandwidth product* has been introduced. The main advantages and disadvantages with respect to other magnetic transducers are given in the paper.

A hardware prototype was realized, and the analytical developments have been verified by means of a reference magnetic field generation system. The experimental tests on the closed-loop transducer show a very good sensitivity, and flux densities in the order of fractions of μT have been usefully sensed in a frequency range up to tens kHz. On the basis of an additional RMS to DC converter and a millivolltmeter, a one-axis gauss meter can be readily obtained.

Useful guidelines for the transducer design are given in the paper, in terms of output current and voltage sensitivity, cut-off frequency and nulling coil parameters.

VII. References

[1] IEEE Std 1460-1996, "IEEE guide for the measurement of quasi-static magnetic and electric fields, 28 Mar 1997.

[2] Lenz, J.E., "A review of magnetic sensors," *Proceedings of the IEEE*, Vol. 78, No. 6, June 1990 , pp. 973-989.

[3] G. Bartington, "Sensors for low level low frequency magnetic fields," *IEE Colloquium on Low Level Low Frequency Magnetic Fields*, 1994, pp. 2/1-2/9.

[4] F. Primdahl, "The fluxgate magnetometer," *J. Phys. E: Sci. Instrum.*, vol. 12, 1979, pp. 241-253.

[5] R.J. Parker, J.C. Nowlan, "Effective magnetic measurements," in *Proc. of Electrical Electronics Insulation Conference and Electrical Manufacturing & Coil Winding Conference*, Chicago, 1993, pp. 215-219.

[6] G. Caruntu, O. Dragomirescu, "The nonlinearity of magnetic sensors," in *Proceedings of Intl. Semiconductor Conference*, CAS 2001, Vol. 2, pp. 375-378.

[7] J. Sedgwick, W.R. Michalson, R. Ludwig, "Design of a digital gauss meter for precision magnetic field measurements," *IEEE Trans. Instrumentation and Measurement*, Vol. 47, No. 4, Aug. 1998, pp. 972-977.

[8] J.M. Dias Pereira, O. Postolache, P.M.B. Silva Girao, "A temperature-compensated system for magnetic field measurements based on artificial neural networks," *IEEE Trans. Instrumentation and Measurement*, Vol. 47, No. 2, April 1998, pp. 494-498.

[9] IEEE Std 1308-1994, "IEEE recommended practice for instrumentation: specifications for magnetic flux density and electric field strength meters - 10 Hz to 3 kHz," 25 April 1995.

[10] W.M. Frix, G.G. Karady, B.A. Venetz, "Comparison of calibration systems for magnetic field measurement equipment," *IEEE Trans. Power Delivery*, Vol. 9, No. 1, Jan. 1994, pp. 100-108.